PHYSICAL REVIEW B, VOLUME 65, 180503(R)

Direct observation of a threshold for coherent radiation in unshunted Josephson-junction arrays with ground planes

B. Vasilić,[1,*] P. Barbara,[2] S. V. Shitov,[3] and C. J. Lobb[1]
[1]*Center for Superconductivity Research, Department of Physics, University of Maryland, College Park, Maryland 20742*
[2]*Department of Physics, Georgetown University, Washington, DC 20057-0995*
[3]*IREE, Russian Academy of Sciences, Mokhovaya 11/7, 101999 Moscow, Russia*
(Received 8 January 2002; published 23 April 2002)

Previous experiments [Barbara *et al.*, Phys. Rev. Lett. **82**, 1963 (1999); Vasilić *et al.*, Appl. Phys. Lett. **78**, 1137 (2001)] showed that two-dimensional, unshunted Josephson-junction arrays emit radiation coherently when a threshold number of junctions is switched to a radiating state. Here, we report low-power radiation being emitted when the number of radiating junctions is smaller than the threshold number. We show that in this regime the output power is incoherent, i.e., the array behavior is qualitatively different from the coherent regime.

DOI: 10.1103/PhysRevB.65.180503 PACS number(s): 74.50.+r, 85.25.Cp, 07.57.Hm, 42.60.Da

If V is the voltage across a Josephson junction, γ the gauge invariant phase difference, I_C the critical current and Φ_0 the flux quantum, the Josephson relations

$$V=\frac{\Phi_0}{2\pi}\frac{d\gamma}{dt} \quad \text{and} \quad I=I_C\sin(\gamma) \tag{1}$$

predict that if there is constant voltage the current will oscillate with a frequency proportional to that voltage. Utilizing this unique property, for the last two decades Josephson-junction arrays (JJA) have been studied as microwave sources.[1] The advantages of using arrays as opposed to junctions are higher power outputs and better impedance matching to typical loads. Arrays used as radiation sources[2–4] were shunted, thus nonhysteretic, which provided tunability to the output radiation. Because of the nonhysteretic nature of the current-voltage (IV) characteristic, all the junctions in these arrays are always oscillating.

In contrast to this standard approach, our previous work[5,6] explored unshunted *hysteretic* JJA that produced millimeter-wave radiation at a frequency fixed by a resonance. The hysteresis enabled us to control the number of radiating junctions. By studying the radiation output of these arrays as a function of the number of radiating junctions, we observed that a certain threshold number of oscillating junctions was necessary for the array to emit coherently. Below this threshold no power could be detected.

In this work we present more sensitive measurements that reveal that our arrays radiate even when the number of radiating junctions is below the threshold number. However, a qualitative change is observed when the number of radiating junctions is increased above the threshold.

Our arrays are made of unshunted $Nb/AlO_x/Nb$ junctions[6] and there is a ground plane above each of the arrays. At one end of each array there is a detector circuit to measure radiation from the array. The other end is shorted to the ground plane. The arrays are current biased and we define rows to be perpendicular to the bias current. Even though these devices are essentially operating at a single frequency, the high efficiencies (up to 32% from dc to 165 GHz[6]), significant power outputs and the control over the number of active junctions make them interesting for further study.

While shunted JJA arrays are tunable over various ranges of frequency[7] our unshunted arrays work in a completely different manner.[5,6] The critical current of each junction with no applied magnetic field is about 150 μA. If we suppress the critical current to about 15 μA by applying a magnetic field parallel to the array, resonant features appear in the IV characteristic. These features are sharp, equally spaced in voltage, self-induced resonant steps (SIRS).[5]

Because of the hysteresis, for currents below the critical current each row can have either no voltage drop across it (the supercurrent branch) or it can have the resonance voltage ($V_{res}\approx 330$ μV) across it (the SIRS). The steps shown in Figs. 1(a) and 2(a), correspond to different numbers of rows being switched to this new state. The ground planes are essential for the operation of our arrays, since the SIRS exist only when there is a ground plane above or below the array. The SIRS are a result of a resonant effect where the junctions pump power at a frequency determined by the resonant cavity formed by the array and the ground plane. Only when we bias the array on these steps does it emit power, at a frequency that corresponds to the resonance voltage $f_{res}=V_{res}/\Phi_0$ through the Josephson relation. We shall stress the two main features of our arrays that are important in their own right, and are absent in the standard unshunted JJA:

(a) Because of the highly hysteretic IV characteristic of our arrays we can switch a desired number of rows onto an SIRS. This gives us control over the number of radiating oscillators in our devices, as opposed to shunted JJA, where *all* junctions are always in the oscillating, nonzero voltage state. A row that is biased on a SIRS will be called *active*, while a row biased on the supercurrent or resistive branch will be called *inactive*;

(b) Once the array is biased on an SIRS we can control the input dc power by varying the dc bias current. This feature allows us to examine the array operation for different input powers with the number of active rows being fixed.

In order to better understand the radiating state we measured the output power P_{AC} as a function of the input power

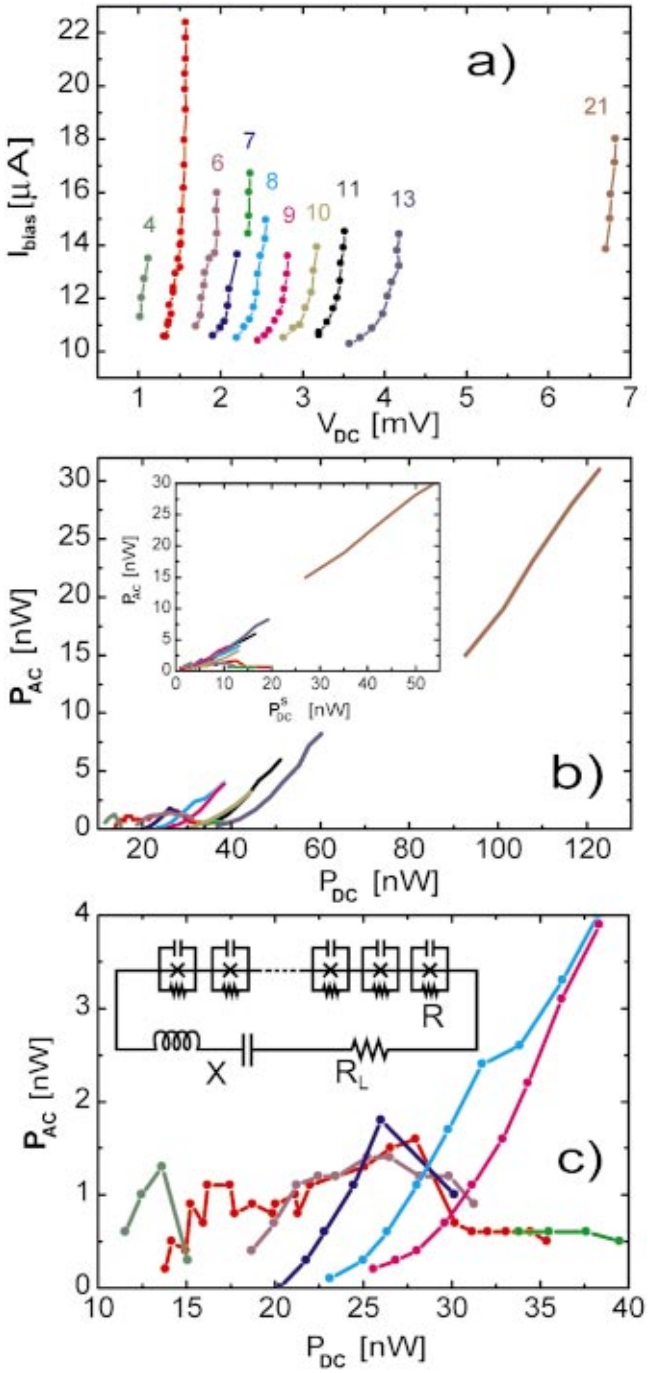

FIG. 1. (Color) (a) Current-voltage characteristics and corresponding (b) output P_{AC} vs input P_{DC} power curves are shown for an array with two columns and 36 rows. The numbers of active rows to which certain self-induced resonant steps correspond are marked and color coded on the *IV* characteristics. For example, the red curves on all graphs in this figure correspond to five active rows. (c) Enlargement of the low dc power region, showing steps number 4 through 9. The inset in (b) shows P_{AC} as a function of the dc power, P_{DC}^S supplied only to the supercurrent channel. The inset in (c) is a schematic of a simple model of the arrays.

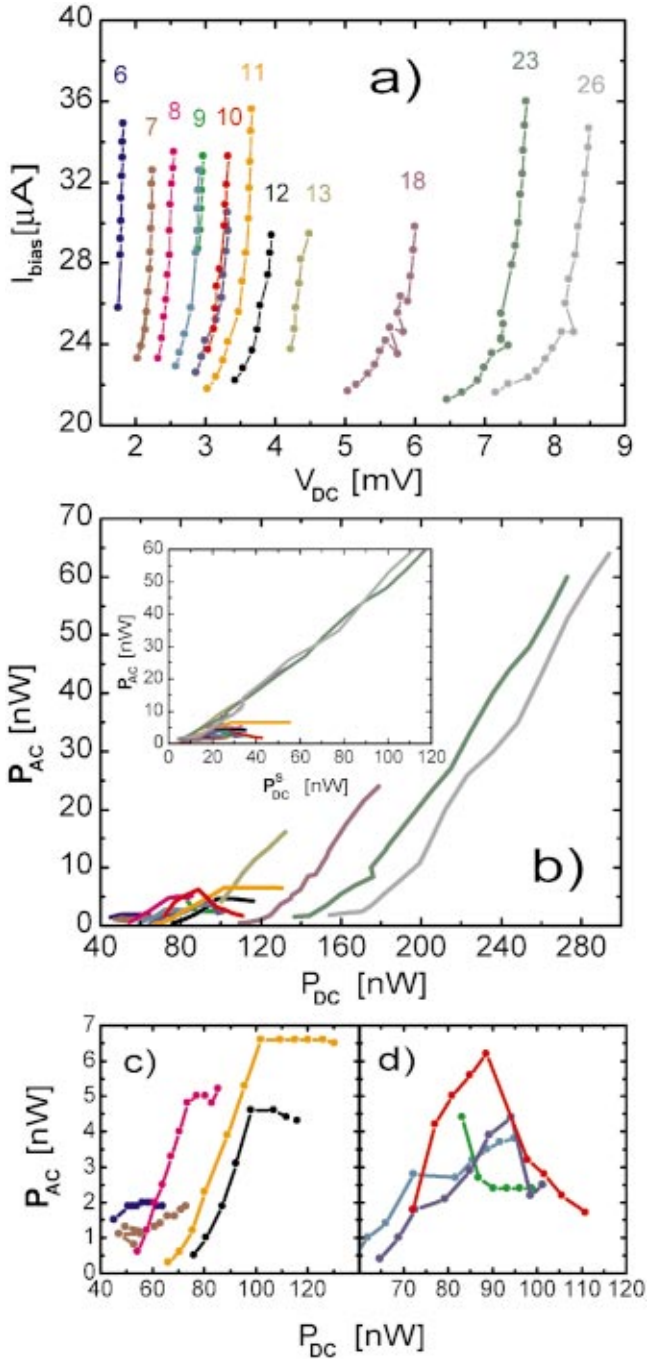

FIG. 2. (Color) Graphs (a) and (b) show plots analogous to the ones shown in Fig. (1) for an array with four columns and 36 rows. The color coding is different. Graphs (c) and (d) are enlargements of the low power region. The plot in (c) shows steps number 6, 7, 8, 11, and 12. For all of them P_{AC} saturates as a function of P_{DC}. The plot in (d) shows steps 9 and 10. Each step has two data sets corresponding to it. For both steps the two data sets display different P_{AC} vs P_{DC} dependences.

P_{DC} for a fixed number of active rows. After biasing on a given SIRS, corresponding to N_A active rows, by varying the bias current we could vary the input power $P_{DC} = I_{bias} V_{DC}$. For each point in Figs. 1 and 2 we recorded the bias current, the dc voltage at that bias current, and the cor-

responding *IV* characteristic of the detector circuit. The power radiated by the array could be estimated by numerically modeling the photon-assisted tunneling process in the detector circuit.

For each SIRS, data were taken consecutively: Once we biased near the bottom/top of the step, we would increase/decrease the bias current and take data, making sure that the array stayed in the same dynamical state.

Before we analyze the data let us see what one would expect from an array in which all the junctions are frequency locked. We will assume that the frequency is independent of the bias current, which is a good approximation when the array is biased on the very steep, top part of the SIRS's. For simplicity, we will consider a one-dimensional array of N identical junctions, shown in the inset in Fig. 1(c), connected in series with a load of impedance $Z=R_L+iX$. Each junction carries a dc bias current I_{bias} that gets split into a resistive channel, representing the quasiparticle leakage I_R, and into a supercurrent channel, which supports a dc, I_S, current because of the resonant effect. Also, there will be an ac current flowing through the junction. We assume that each active junction has a dc voltage V_{DC}/N_A across it, where N_A is the number of active junctions, and that all junctions have an ac component with amplitude V_{AC} and a phase shift δ_n. We assume the phase shifts δ_n to be different from junction to junction while restricting V_{AC} to be constant.

The bias current supplies the system with dc power equal to $V_{DC}I_R+V_{DC}I_S$. The first term is the dc power dissipated in the resistors. The second term is the dc power P^S_{DC} that gets converted into ac power, which we will denote with P^S_{AC} that is, $P^S_{AC}=P^S_{DC}$. There are only two sources of dissipation in the system, the junction resistors and the load. Following this power conservation argument, we find that the total ac power supplied to the system, P^S_{AC}, has to be completely dissipated in the junction resistors, P^R_{AC}, and in the load resistor as P_{AC} that is our measured power. We are interested in how P^S_{AC} is distributed between the power dissipated in the array, P^R_{AC}, and the power dissipated in the load, P_{AC}, and how this distribution depends on the relative phases of the junctions. Assuming harmonic time dependence of the voltages across the junctions and using power conservation, we obtain

$$P^S_{DC}=P^S_{AC}=P^R_{AC}+P_{AC}=\frac{NV^2_{AC}}{2R}+\langle V_L I_L\rangle, \tag{2}$$

$$P^S_{DC}=P^S_{AC}=N\frac{V^2_{AC}}{2R}+\xi N^2\frac{V^2_{AC}}{2R_{eff}}, \tag{3}$$

where $\langle\cdots\rangle$ denotes a time average over one period, V_L and I_L are the voltage across the load resistor and the current through it, with the following definitions of the effective resistance R_{eff} and the coherence factor ξ:

$$R_{eff}=R_L\left(1+\frac{X^2}{R_L^2}\right), \quad \xi=\frac{1}{N^2}\sum_{n,m=1}^{N}\cos(\delta_n-\delta_m). \tag{4}$$

From Eq. (3) we solve for the ac amplitude V_{AC} as a function of the input dc power,

$$V_{AC}=\sqrt{\frac{1}{\frac{N}{2R}+\frac{\xi N^2}{2R_{eff}}}P^S_{DC}}. \tag{5}$$

Substituting this expression only in the term for P^R_{AC} in Eq. (2) and solving for P_{AC} we get

$$P_{AC}=\frac{1}{1+\frac{1}{\xi}\frac{R_{eff}}{NR}}P^S_{DC}. \tag{6}$$

As mentioned before, this derivation assumes frequency locking of the junctions. In the case in which the junctions are also phase locked, ξ is constant and Eq. (6) implies that P_{AC} is a linear function of P^S_{DC}. If the phases are scrambled, making ξ smaller, the slope of this dependence is smaller and vice versa. For a given junction resistance and load impedance the distribution of a given input power P^S_{DC} depends only on the relative phases of the oscillating voltages across the junctions. For example, for a fixed P^S_{DC}, if ξ is decreased, decreasing the power delivered to the load, V_{AC} will grow, as given in Eq. (5), to increase the dissipation in the junction resistors and satisfy power conservation in Eq. (3). This argument does not depend on the particular wave form of the oscillating voltage across the junctions, so it is model independent.

We recorded P_{AC} vs $P_{DC}=I_{bias}V_{DC}$ curves for different numbers of active rows in different arrays. We should note that P_{DC} includes the quasiparticle dissipation as opposed to P^S_{DC} that is only the supercurrent dc power. Since the SIRS are fairly steep, and the subgap resistance large, P^S_{DC} and P_{DC} differ by an approximately constant power when we are biasing along a single step. Figures 1 and 2 show P_{AC} vs P_{DC} curves and their corresponding *IV* curves for two arrays with 36 rows, one two-columns wide and the other four-columns wide.

There are two striking properties of the P_{AC} vs P_{DC} functions. First, when the number of active rows is low, the output power saturates and does not grow with the input power. For a large number of active rows the output power always grows with the input power and becomes linear for high powers. We define the *threshold*[8] as the number of active rows where this qualitative change in the P_{AC} vs P_{DC} dependence occurs. For the array with two columns the threshold is eight rows and for the array with four columns it is 13 rows. As mentioned previously, only at high powers the dc voltage (ac frequency) becomes nearly independent of the bias current and we can use Eq. (6) to conclude that the arrays then become phase locked. The insets in Figs. 1(b) and 2(b) show P_{AC} as a function of P^S_{DC}, with $P^S_{DC}=V_{DC}(I_{bias}-I_R)$. We estimate I_R as the quasiparticle leakage current obtained from the *IV* characteristics. All the curves above threshold lie on the same line as predicted by Eq. (6), while the ones below threshold lie below this linear dependence indicating loss of coherence.

The threshold transition is shown in Figs. 1(c), 2(c), and 2(d). For example, even though on step number 11 in Fig. 2(c) the input power reaches levels similar to when the array is biased on step number 13, P_{AC} is much lower and does not show the same dependence on P_{DC}. For these small number of active junctions, the output power often decreases when the input power increases.

We have also noticed that below threshold, the power output on given bias points is not always the same. This is the case with steps number 9 and 10, shown in Fig. 2(d). For each of these two SIRS there are two overlapping sets of points in the *IV* characteristic. However, the power dependence for these two sets is completely different, as the P_{AC} vs P_{DC} plot shows. This means that the junctions had different relative phases each time we biased changing the power delivered to the load.

Second, even though there is a drastic change in the amount of power that the array is delivering to the detector, the steps in the *IV* characteristic do not show any change going from below to above threshold. Both the step height (in current) and shape remain approximately the same as shown in Figs. 1 and 2. For example, step number 5 in Fig. 1(a) reaches bias currents greater than any of the bias currents at which the other steps exist. Yet, the array radiates five times more ac power when biased on step number 9, compared to when it is biased on step number 5, for the same input dc power of 35 nW.

There is extensive theoretical work describing the interaction of single junctions and arrays with resonant cavities.[9–14] The most recent work[15–18] is aimed toward understanding experimental results[5,6] on underdamped arrays. Theory has provided descriptions of frequency locking to a cavity,[15,16] array *IV* curves that can be compared with experiment,[15,17] and descriptions of the coherent radiating state,[15–17] including the degree of coherence[16,17] and power along a given step as I_{bias} is varied.[17] Theory has thus successfully reproduced most of the observed phenomena. As discussed by Barbara *et al.*,[17] however, one outstanding problem remains.

The most recent theory predicts coherent radiation as soon as the array is biased on a SIRS, that is, there is no threshold for coherent radiation. By contrast, our experiments show distinctly different behavior below and above threshold, as discussed above and in our previous work.[5] The task remaining for theory is to explain the threshold, and to characterize the degree of coherence and the radiation output both above and below threshold.

This work was supported by the AFOSR under Grant No. F49620-98-1-0072.

*Email address: brana@umd.edu

[1] M. Darula, T. Doderer, and S. Beuven, Supercond. Sci. Technol. **12**, R1 (1999).

[2] S.P. Benz and C.J. Burroguhs, Appl. Phys. Lett. **58**, 2162 (1991).

[3] A.K. Jain, K.K. Likharev, J.E. Lukens, and J.E. Sauvageau, Phys. Rep. **109**, 309 (1984).

[4] R.S. Newrock, C.J. Lobb, U. Geigenmüller, and M. Octavio, Solid State Phys. **54**, 263 (2000).

[5] P. Barbara, A.B. Cawthorne, S.V. Shitov, and C.J. Lobb, Phys. Rev. Lett. **82**, 1963 (1999).

[6] B. Vasilić, S.V. Shitov, C.J. Lobb, and P. Barbara, Appl. Phys. Lett. **78**, 1137 (2001).

[7] P. Hadley, M.R. Beasley, and K. Wiesenfeld, Phys. Rev. B **38**, 8712 (1988).

[8] In our earlier measurements the sensitivity of the output power measurements was lower and we could not detect output power below threshold. The data was also taken only at one bias current for each different number of active rows, so we only sampled one point on each of the P_{AC} vs P_{DC} curves.

[9] N.R. Werthamer, Phys. Rev. **147**, 255 (1966).

[10] R. Bonifacio, F. Casagrande, and M. Milani, Phys. Lett. **101A**, 427 (1984).

[11] M.O. Scully and P.A. Lee, Phys. Rev. Lett. **22**, 23 (1969).

[12] M.J. Stephen, Phys. Rev. **182**, 531 (1969).

[13] M.J. Stephen, Phys. Rev. Lett. **21**, 1629 (1968).

[14] D.R. Tilley, Phys. Lett. **33A**, 205 (1970).

[15] E. Almaas and D. Stroud, Phys. Rev. B **63**, 144522 (2001).

[16] G. Filatrella, N.F. Pedersen, and K. Wiesenfeld, Phys. Rev. E **61**, 2513 (2000).

[17] P. Barbara, G. Filatrella, C. J. Lobb, and N. F. Pedersen, in *Studies of High Temperature Superconductors* (NOVA Science Publishers, New York, in press).

[18] J.K. Harbaugh and D. Stroud, Phys. Rev. B **61**, 14 765 (2000).